Parity quantum numbers in the density matrix renormalization group

Yu-Chin Tzeng（曾郁欽）*
Department of Physics, National Taiwan University, Taipei 106, Taiwan and
Center of Theoretical Sciences, National Taiwan University, Taipei 106, Taiwan
(Received 22 November 2011; revised manuscript received 26 May 2012; published 5 July 2012)

In strongly correlated systems, numerical algorithms taking parity quantum numbers into account are used not only for accelerating computation by reducing the Hilbert space but also for particular manipulations such as the level spectroscopy (LS) method. By comparing energy differences among different parity quantum numbers, the LS method is a crucial technique used in identifying quantum critical points of Gaussian and Berezinsky-Kosterlitz-Thouless– (BKT) type quantum phase transitions. These transitions that occur in many one-dimensional systems are usually difficult to study numerically. Although the LS method is an effective strategy to locate critical points, it has lacked an algorithm that can manage large systems with parity quantum numbers. Here a parity density matrix renormalization group (DMRG) algorithm is discussed. The LS method is used with the DMRG in the $S = 2$ XXZ spin chain with uniaxial anisotropy. Quantum critical points of BKT and Gaussian transitions can be located well. Thus, the LS method becomes a very powerful tool for BKT and Gaussian transitions. In addition, Oshikawa's hypothesis in 1992 on the presence of an intermediate phase in the present model is supported by DMRG.

DOI: 10.1103/PhysRevB.86.024403 PACS number(s): 05.10.Cc, 02.70.−c, 75.10.Pq

I. INTRODUCTION

In one-dimensional (1D) quantum many-body systems, Berezinsky-Kosterlitz-Thouless– (BKT)[1] and Gaussian-type quantum phase transitions are usually difficult to study numerically. Methods for accurate determination on the BKT and Gaussian critical points have been proposed.[2–7] However, precise detections from entanglement entropy need to compute on very large size ($N > 10\,000$) systems,[6] and detections from bipartite fluctuations need the preliminary knowledge of Luttinger parameters.[7] The level spectroscopy (LS) method[8,9] based on the sine-Gordon theory is an old method for the BKT- and Gaussian-type quantum phase transitions. By comparing different excitation energies, the LS method is able to detect the Gaussian and BKT critical points accurately. Ground-state phase diagrams have been studied by use of the LS method in many models.[10–14] However, implementation of the LS method usually needs precise energy eigenvalues with parity quantum numbers $p = \pm 1$. Although parity or space inversion is usually a good quantum numbers in condensed matter physics, the exact diagonalzation (ED)[15] was the only accurate numerical algorithm with parity quantum numbers. Therefore, the finite-size effect usually interferes with the LS method because of the limited sizes in ED. In order to avoid the finite-size effect in some difficult cases,[14,16] a precise algorithm with large sizes and parity quantum numbers is now urgently needed.[17]

The density matrix renormalization group (DMRG)[18–21] is a powerful numerical method of strongly correlated systems in 1D and two-dimensional (2D) lattices. Lattice size in DMRG usually achieves hundreds of sites with high accuracy. Recent study on spin-1/2 system in the Kagome lattice revealed that DMRG may be the most accurate numerical method in frustrated 2D systems.[22] Symmetry also plays an important role in DMRG. $U(1)$ symmetry, such as conservation of number of particles and the z component of total spin, is most frequently employed. Non-Abelian symmetry[23] and other descrete symmetries[24,25] are often more complicated and rather difficult to implement. For the parity symmetry, DMRG faces intrinsic difficulties in the algorithm. The core problem of parity in DMRG is that the algorithm divides superblock into left and right parts. This division destroys the spacial inversion if the length of left and right blocks are not equal. When they are equal, for example, in the *infinite-system DMRG*, parity can be utilized.[24] However, *finite-system DMRG* or the so-called *sweeping procedure* is usually needed for obtaining precise energies with a reliable error estimate. In this case, parity is difficult to utilize.

In this paper, parity quantum numbers $p = \pm 1$ in the sweeping procedure are discussed in an alternative ladder scheme. The new method is very simple and no prior knowledge of group theory is required. Therefore, the LS method overcomes the limitation of small sizes in ED and becomes a very powerful tool in detecting BKT and Gaussian transitions. In the state-of-the-art of DMRG, the matrix-product state (MPS)[26] is used mainly for variational algorithms.[27] However,

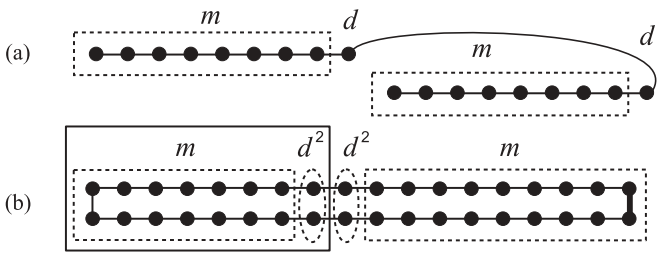

FIG. 1. (a) Parity DMRG scheme proposed by Sørensen.[24] The left and right blocks must be the same size. Parity quantum numbers are available only in the infinite-system DMRG within this scheme. m is the dimension of a block and d is the dimension of a site. (b) Ladder scheme for parity quantum numbers in the sweeping procedure. The left dashed rectangle represents the system block and the solid rectangle represents the enlarged system block. The dimension of one site (dash ellipse) becomes d^2. The bold bond controls the boundary conditions. Thus, accurate results within open, periodic, and twisted boundary conditions can be easily obtained.

in this paper, the parity quantum numbers are discussed in the traditional DMRG, since it continuously shows the significance in the studies.[22,28] In the following section, the trick is discussed in the $S = 1/2$ XXZ model. In Sec. III A, the proposed parity DMRG is applied to perform the LS method in the $S = 2$ XXZ model with uniaxial anisotropy. The BKT and Gaussian transitions are both located precisely. Thus, in Sec. III B, the boundaries of the intermediate-D phase are determined. In other words, the presence of the intermediate-D phase, which Oshikawa predicted 20 years ago,[29] is now supported by DMRG. The conclusions are summarized in Sec. IV.

II. PARITY DMRG

Consider the $S = 1/2$ XXZ model,

$$H = \sum_{j=1}^{N} \frac{1}{2}(S_j^+ S_{j+1}^- + S_j^- S_{j+1}^+) + \lambda S_j^z S_{j+1}^z, \tag{1}$$

where λ is the anisotropic parameter and N is total number of spins. In developing numerical methods of strongly correlated systems, this model can be regarded as a basic testing model[15,18] because the dimension of one site $d = 2$ and it can be solved by using the Bethe ansatz.[30,31] The model undergoes a BKT quantum phase transition at $\lambda_c = 1$. Ground-state energy per site at this critical point in the thermodynamic limit is $e_0 = -\ln 2 + \frac{1}{4}$. Parity quantum numbers of the finite-size ground state and first excited state depend on N. When $L = N/2$ is even (odd), the parity of the ground state is also even (odd) and the first excited state is odd (even). These two states become the twofold degenerate ground state in the thermodynamic limit.

The reason that quantum numbers of S_{tot}^z can be utilized is the fact that the reduced density matrix of the enlarged system block ρ_{sys} and the z component of total spin of the enlarged system block S_{sys}^z are compatible, i.e., $[\rho_{\text{sys}}, S_{\text{sys}}^z] = 0$. Thus, each eigenstate of the reduced density matrix has a quantum number of S_{sys}^z, and these quantum numbers can be used for the next iteration. However, the parity operator $\mathcal{P}$ is a global operator which acts only on the whole chain, the superblock. It is impossible in the original scheme to have an operator $\mathcal{P}_{\text{sys}}$ which only acts on the enlarged system block.

In order to make it possible, the ladder scheme should be employed. As shown in Fig. 1(b), the chain is folded as a two-leg ladder. Now the global parity operator $\mathcal{P}$ can be regarded as an operation of exchanging legs. Moreover,

$$\mathcal{P} = \prod_{i=1}^{L} \mathcal{P}_i, \tag{2}$$

where $L = N/2$ and each $\mathcal{P}_i$ only exchanges legs of rung i. Thus, $\mathcal{P}_{\text{sys}}$ is the parity operator which only exchanges legs of the enlarged system block and $[\rho_{\text{sys}}, \mathcal{P}_{\text{sys}}] = [S_{\text{sys}}^z, \mathcal{P}_{\text{sys}}] = [\rho_{\text{sys}}, S_{\text{sys}}^z] = 0$. The eigenstates of the reduced density matrix have both quantum numbers of S_{sys}^z and $\mathcal{P}_{\text{sys}}$ which can be used for the next iteration in the sweeping procedure. The bases of a rung, the dashed ellipse in Fig. 1(b), are $|\tau_i\rangle \in \{|\uparrow\uparrow\rangle, |\uparrow\downarrow\rangle, |\downarrow\uparrow\rangle, |\downarrow\downarrow\rangle\}$. Each $|\tau_i\rangle$ is an eigenstate of S_i^z; however, these bases are not eigenstates of the parity $\mathcal{P}_i$. Since $[\mathcal{P}_i, S_i^z] = 0$, one can easily find the basis set $\{|\sigma_i\rangle\}$ which is the mutual eigenstates of $\mathcal{P}_i$ and S_i^z,

$$|\sigma_i\rangle \in \left\{ \frac{|\uparrow\downarrow\rangle - |\downarrow\uparrow\rangle}{\sqrt{2}}, \frac{|\uparrow\downarrow\rangle + |\downarrow\uparrow\rangle}{\sqrt{2}}, |\uparrow\uparrow\rangle, |\downarrow\downarrow\rangle \right\}. \tag{3}$$

These states are the so-called singlet and triplet states with corresponding quantum numbers of parity $p_i = -1, 1, 1$, and 1, respectively, and quantum numbers of the z component of spin $s_i^z = 0, 0, 1$, and -1, respectively. Equation (2) implies the quantum number of the enlarged system block $p_k = p_l p_n$, where p_l is quantum number of the system block and p_n is the quantum number of a single rung. These indexes satisfy the relation $k = (l-1)d^2 + n$.

The $\{|\sigma_i\rangle\}$ forms a transformation matrix Q,

$$Q = \begin{pmatrix} 0 & 0 & 1 & 0 \\ \frac{1}{\sqrt{2}} & \frac{1}{\sqrt{2}} & 0 & 0 \\ \frac{-1}{\sqrt{2}} & \frac{1}{\sqrt{2}} & 0 & 0 \\ 0 & 0 & 0 & 1 \end{pmatrix}. \tag{4}$$

The spin operators of the first and second sites of rung i are $S_{1,i}^z = Q^T(S^z \otimes 1_{d\times d})Q$, $S_{2,i}^z = Q^T(1_{d\times d} \otimes S^z)Q$, $S_{1,i}^+ = Q^T(S^+ \otimes 1_{d\times d})Q$, $S_{2,i}^+ = Q^T(1_{d\times d} \otimes S^+)Q$, $S_{1,i}^- = Q^T(S^- \otimes 1_{d\times d})Q$, and $S_{2,i}^- = Q^T(1_{d\times d} \otimes S^-)Q$. $1_{d\times d}$ is a $d \times d$ identity matrix. The two spins of the first rung interact with each other in the ladder scheme. The Hamiltonian of the first rung H_1 is a $d^2 \times d^2$ matrix and it is fortunately already diagonalized with the eigenvalue $\frac{-2-\lambda}{4}$ for the singlet state and the eigenvalues $\frac{2-\lambda}{4}$, $\frac{\lambda}{4}$, and $\frac{\lambda}{4}$ for the triplet states, respectively. The Hamiltonian of the latest rung H_L, the bold bond shown in Fig. 1(b), can be flexible chosen as different boundary conditions. For example, $H_L = H_1 = \text{diag}(\frac{-2-\lambda}{4}, \frac{2-\lambda}{4}, \frac{\lambda}{4}, \frac{\lambda}{4})$ is the periodic boundary condition (PBC), $H_L = 0$ is the open boundary condition (OBC), and $H_L = \text{diag}(\frac{2-\lambda}{4}, \frac{-2-\lambda}{4}, \frac{\lambda}{4}, \frac{\lambda}{4})$ is the twisted boundary condition (TBC). Thus, Eq. (1) can be rewritten as

$$H = \sum_{\alpha=1}^{2} \sum_{i=1}^{L-1} \frac{1}{2}(S_{\alpha,i}^+ S_{\alpha,i+1}^- + S_{\alpha,i}^- S_{\alpha,i+1}^+) + \lambda S_{\alpha,i}^z S_{\alpha,i+1}^z + H_1 + H_L, \tag{5}$$

where $L = N/2$. Once a DMRG programmer has above information, the DMRG with parity quantum numbers can be performed. The energies of ground state and first excited state with corresponding parity quantum numbers are listed in Table I and plotted in Fig. 2 for looking at convergence of energy with respect to system size.

TABLE I. Energy per site of 1D spin-1/2 XXZ model. p_0 and p_1 are parity quantum numbers of the ground state and first excited state, respectively. The number of state kept in the largest size is up to $m = 1500$ and the truncation error is of the order 10^{-9}. Three sweeps are performed. The periodic boundary condition is used here, i.e., $H_1 = H_L = \text{diag}(\frac{-2-\lambda}{4}, \frac{2-\lambda}{4}, \frac{\lambda}{4}, \frac{\lambda}{4})$ in Eq. (5).

N	λ	p_0	E_0/N	p_1	E_1/N
54	1	$-$	-0.44343001	$+$	-0.44189435
100	1	$+$	-0.44322957	$-$	-0.44277665
162	1	$-$	-0.44317856	$+$	-0.44300474

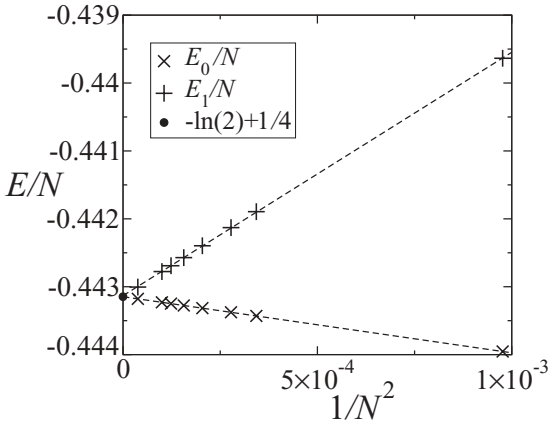

FIG. 2. The ground-state and first-excited-state energy per site of spin-$\frac{1}{2}$ Heisenberg model, i.e., $\lambda = 1$ in Eq. (5). PBC is used and three sweeps are performed in parity DMRG. The dot indicates the exact ground-state energy in the thermodynamic limit from the Bethe ansatz.

Although parity reduces the dimension of superblock by a factor 2, the disadvantage of the ladder scheme is the dimension of one site becomes squared. In other words, 4 in the $S = 1/2$ chain, 9 in the $S = 1$ chain or the t-J model, 16 in the Hubbard model, and 25 in the $S = 2$ chain. The overall computational difficulty increases, especially when d is very large. One can further use single center site[20] to reduce the dimension of superblock. As mentioned by White, the ladder scheme is a better configuration for PBC but it only improves convergence with the number of sweeps.[20] I emphasize the feasibility of parity DMRG in the ladder scheme. Thus, in the case $d^2 = 25$, the $S = 2$ XXZ model with uniaxial anisotropy is examined in Sec. III as practical examples. DMRG with a single center site[20] is not employed here. In addition to quantum numbers ($S^z_{\rm tot}$ and $\mathcal{P}$), the only optimization in this work is the *wave-function transformation*[19] which was proposed by White in 1996 and has become a standard optimization in performing DMRG.

III. $S = 2$ XXZ MODEL WITH UNIAXIAL ANISOTROPY

$S = 2$ spin chains are research topics of current interest, including topological phases and quantum phase transitions,[14,32–37] magnetization processes,[38] and cold atoms loaded into a 1D optical lattice.[39] The $S = 2$ XXZ model with uniaxial anisotropy is defined by

$$H = \sum_{j=1}^{N} \left(S^x_j S^x_{j+1} + S^y_j S^y_{j+1} + \lambda S^z_j S^z_{j+1} \right) + D \sum_{j=1}^{N} \left(S^z_j \right)^2, \tag{6}$$

where λ and D are the XXZ anisotropy parameter and uniaxial anisotropy parameter, respectively. This model exhibits a Haldane gap in the Haldane phase with a nonlocal string order.[40,41] Although the ground-state phase diagram for the entire parameter space is unclear, it is expected to have Haldane, Néel, large-D, intermediate-D, XY1, XY4, and ferromagnetic phases. Quantum phase transitions with various universality classes are in this model. It is still a controversial issue[14,29,32,42–44] whether the intermediate-D (ID) phase hypothesized by Oshikawa[29] 20 years ago exists in ground-state phase diagram. Although by use of the DMRG the ID phase was absent,[42–44] surprisingly, by using ED to perform LS on very small sizes ($N \leqslant 12$), Tonegawa *et al*. obtained the ID phase in a very narrow region. However, the ED estimations may not reveal the results of the thermodynamic limit because of the finite-size effect, especially when $D > 2$. Energy-level crossing does not appear in small sizes at all. The region of the phase diagram that cannot be determined by ED was, thus, determined by extrapolation of phase boundaries.[14]

A. Level spectroscopy method

Therefore, the first application of the parity DMRG is to perform the LS method by focusing on the BKT transition from the XY1 to the large-D phase as well as the Gaussian transitions from the large-D to the ID phase and the ID to the Haldane phase. Following the LS method, these three excitation energies, $E_0(N,0,+;\text{tbc})$, $E_0(N,0,-;\text{tbc})$, and $E_0(N,2,+;\text{pbc})$, should be compared, where $E_0(N,M,p;\text{tbc})$ and $E_0(N,M,p;\text{pbc})$ denote the lowest-energy eigenvalues of N spins in the subspace of the z component of the total spin M and the parity quantum number p within the TBC and PBC, respectively.

The BKT pseudocritical points of XY1–large-D satisfy the condition[14]

$$E_0(N,0,+;\text{tbc}) - E_0(N,2,+;\text{pbc}) = 0, \tag{7}$$

and the Gaussian pseudocritical points of large-D–ID and ID–Haldane satisfy the condition[14]

$$E_0(N,0,+;\text{tbc}) - E_0(N,0,-;\text{tbc}) = 0. \tag{8}$$

These pseudocritical points are extrapolated to $N \to \infty$ by assuming the quadratic scaling function of N^{-2} after collecting the finite-size results. Figure 3 demonstrates the LS method for the BKT transitions; $\lambda = 0$ is fixed in Eq. (6). The number of states kept is to $m = 800$, and the truncation error is about 10^{-8}. The BKT quantum phase transitions are usually difficult to precisely locate numerically. However, this critical point is well located by use of the LS method after using the parity DMRG. As shown in Fig. 3(b), the critical

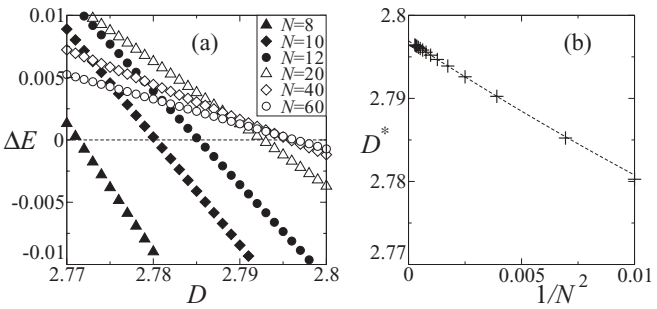

FIG. 3. The LS method for the BKT transition in the model Eq. (6). $\lambda = 0$ is fixed. Energy differences in Eq. (7) with different sizes are shown in (a) and extrapolation of the critical point is shown in (b). $N = 8$, 10, and 12 are computed by ED, and larger sizes are computed by DMRG. Only $N \geqslant 16$ are used for the extrapolation. The XY1–large-D critical point from the extrapolation $D_c = 2.796917 \pm 5 \times 10^{-6}$.

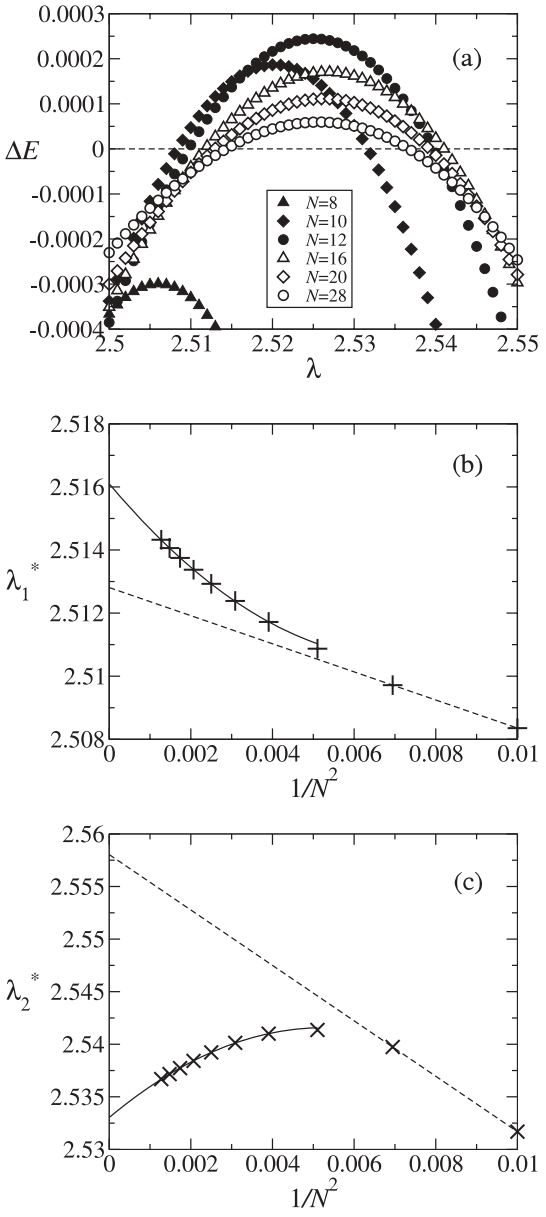

FIG. 4. The LS method for Gaussian transition in model Eq. (6). $D = 2.1$ is fixed. Energy differences in Eq. (8) with different sizes are shown in (a) and the extrapolations of critical points are shown in (b) and (c). $N \leqslant 12$ are computed by ED, and larger sizes are computed by DMRG. Since energy-level crossing takes place when $N \geqslant 10$, it is not sufficient for quadratic fitting with only the ED data. The dash lines in (b) and (c) are linear guild from ED. The solid lines are the extrapolations with only $16 \leqslant N \leqslant 28$. The critical points for large-D–ID and ID-Haldane are $\lambda_{c1} = 2.51610 \pm 3 \times 10^{-5}$ and $\lambda_{c2} = 2.53303 \pm 4 \times 10^{-5}$, respectively.

point $D_c = 2.796917 \pm 5 \times 10^{-6}$ is determined precisely. By comparing the recent accuracy of detecting BKT quantum phase transitions,[7] the LS method becomes a very powerful tool for the study of BKT quantum phase transitions.

For the Gaussian transitions, Fig. 4 shows the LS results with fixed $D = 2.1$. Due to the finite-size effect, the energy-level crossing does not take place until $N \geqslant 10$. Consequently, it is not sufficient for quadratic fitting with only the ED data of $N = 10$ and 12.[14] In fact, the ID-Haldane pseudocritical point λ_2^* behaves nonmonotonically with size. As shown in Figs. 4(b) and 4(c), only $16 \leqslant N \leqslant 28$ are used for the extrapolation. The critical points in the thermodynamic limit are $\lambda_{c1} = 2.51610 \pm 3 \times 10^{-5}$ and $\lambda_{c2} = 2.53303 \pm 4 \times 10^{-5}$ for large-D–ID and ID-Haldane, respectively. The number of states kept is to $m = 1300$ in the largest size, and the dimension is about 5×10^7 in the Lanczos diagonalization of finding the lowest-energy eigenstate. The order of truncation error is 10^{-8} in the worst case. In contrast, recent determinations of the Gaussian transition achieved similar accuracy by considering the entanglement entropy up to 20 000 sites.[6] Therefore, the LS method also becomes a very powerful tool for the Gaussian transitions. In addition, following the LS method, it implies the presence of the ID phase in model of Eq. (6). Thus, Oshikawa's hypothesis in 1992[29] is now supported by DMRG. However, the region of the ID phase in $D = 2.1$ is merely about 0.017. It may explain why the ID phase has not been found from previous DMRG studies consequently.[42–44]

B. Intermediate-D phase boundary

The phase diagram is focused on the region $D \geqslant 2.1$, which has contained some ambiguity in previous studies. A possible scenario is that the ID phase boundaries of ID-Haldane and large-D–ID merge at a point. This point $(\lambda_c, D_c) \simeq (2.64, 2.19)$ was estimated by extrapolation of phase boundaries from $D \lesssim 2$.[14] In this scenario, the Haldane and large-D phases are suggested to be the same phase.[14,37] However, from previous analysis by use of ED,[14] it is known that larger values of D lead the level crossing to begin at a larger size. Therefore, based on the presence of the ID phase, there are two other possible scenarios against the first one. One is that the merge point (λ_c, D_c) is located exactly at the boundary of the Néel phase and becomes a multicritical point. Another possible scenario is that the ID phase extends and reaches the Néel phase. In the latter two scenarios, the Haldane and large-D phases are completely separated by the ID phase and definitely not the same phase, although recent studies have suggested they could be the same phase.[14,37]

Departing from empiric of ED, as shown in Fig. 5 for $D = 2.14$, despite the pseudocritical points satisfy the condition Eq. (8) in small sizes, there is no energy-level crossing in

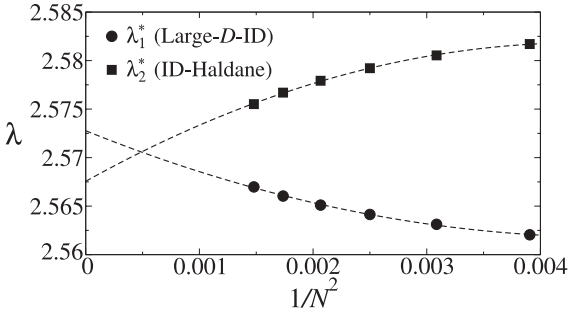

FIG. 5. $D = 2.14$. Although the pseudocritical points satisfy the condition Eq. (8), there is no energy-level crossing in the thermodynamic limit. In other words, there is no Gaussian transition. This strong finite-size effect is not observed[14] until use of this parity DMRG method.

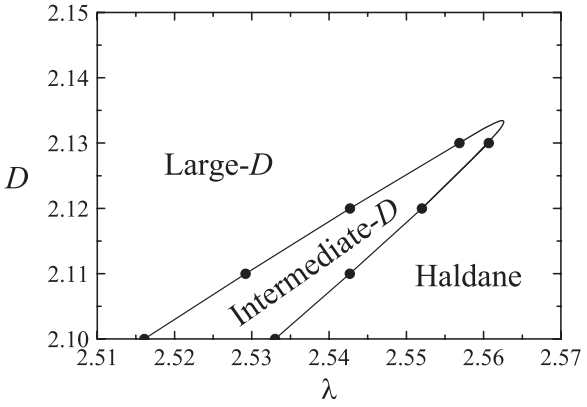

FIG. 6. The phase boundary of the intermediate-D phase in the $S = 2$ XXZ chain with uniaxial anisotropy. The phase boundary lines between the ID and Haldane phases and between the large-D and ID phases merge at a point between $2.13 < D_c < 2.14$.

the thermodynamic limit. In other words, according to the LS method, there is no Gaussian transition, and the scenarios where the ID phase completely separates the Haldane and large-D phases are excluded. The more precise phase diagram by means of the parity DMRG is shown in Fig. 6.

Finally, the accuracy of the current research is carefully examined. It is known that the often-used measure of the error in DMRG calculations, the truncation error, may not reveal the true relative error of energy in the infinite-system DMRG.[24] In the finite-system DMRG, the truncation error is a more reliable indication to the true error. The energies of $\lambda = 2.51$ and $D = 2.1$ for $N = 28$ in Eq. (8) as the number of states kept m increases are listed in Table II. From these data, the absolute errors of energy in Fig. 4(a) are argued to be of order 10^{-6}, and the relative errors to be the same order with the truncation error. Therefore, the energies are sufficiently accurate for distinguishing the energy differences in the current studies. The phase diagram in Fig. 6 thus provides a solid numerical evidence for the presence of the ID phase in the $S = 2$ XXZ chain with uniaxial anisotropy, Eq. (6).

IV. CONCLUSION

The parity (space inversion) quantum numbers are of significance not only in computational advances but also in the LS method. By employing the ladder scheme, the global parity operator can be decomposed into the product

TABLE II. The energies for $N = 28$ in Eq. (8) as m increases. $\lambda = 2.51$ and $D = 2.1$. Three sweeps are performed.

m	$p = +1$	$p = -1$	Truncation error
600	−95.907406036	−95.907356973	5.9×10^{-7}
700	−95.907437223	−95.907385487	2.9×10^{-7}
800	−95.907451123	−95.907399047	1.6×10^{-7}
900	−95.907458008	−95.907405896	9.6×10^{-8}
1000	−95.907461893	−95.907409748	5.8×10^{-8}
1100	−95.907464072	−95.907411938	3.7×10^{-8}
1200	−95.907465368	−95.907413199	2.5×10^{-8}
1300	−95.907466194	−95.907413994	1.7×10^{-8}

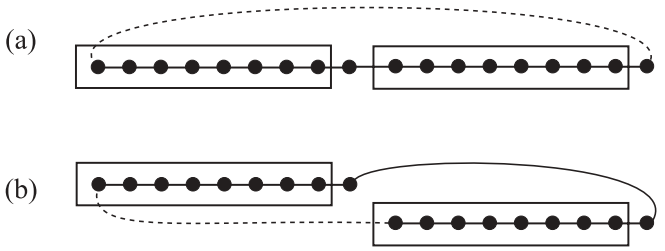

FIG. 7. The old parity schemes in the infinite-system DMRG[24] for (a) the PBC and (b) the TBC. The dashed line shows the boundary coupling. The left and right blocks must be the same length. The truncation error may not reveal the true relative error of energy.[24] It is difficult to evaluate how many states should be kept is enough.

form in Eq. (2). It makes DMRG able to utilize the parity quantum numbers. The LS method is used with DMRG in the $S = 2$ XXZ model with uniaxial anisotropy. The BKT critical point of XY1–large-D as well as Gaussain critical points of large-D–ID and ID-Haldane are determined very precisely. Thus, the LS method is suggested to be the most powerful tool for detecting BKT and Gaussian transitions.

The phase diagram of the $S = 2$ XXZ model with uniaxial anisotropy, Fig. 6, is investigated by focusing on the ID phase boundary where the ED results are strongly affected by the finite-size effect. This work is consistent with previous findings,[14,37] thus providing support to Oshikawa's hypothesis[29] in 1992 regarding DMRG.

Since the proposed method in the case $d^2 = 25$ works well, it is also feasible for a large number of models, including $S = 1/2$ spin chains, $S = 1$ spin chains, the t-J model, the Hubbard model, topological interacting fermion systems,[16] and ladders.

ACKNOWLEDGMENTS

I am grateful to Ying-Jer Kao, Min-Fong Yang, Hsiang-Hsuan Hung, Wei-Chao Shen, Hsiao-Ting Tzeng, and Hui-Chen Tsai for discussions and encouragement. I am also grateful to Takashi Tonegawa for discussions about the

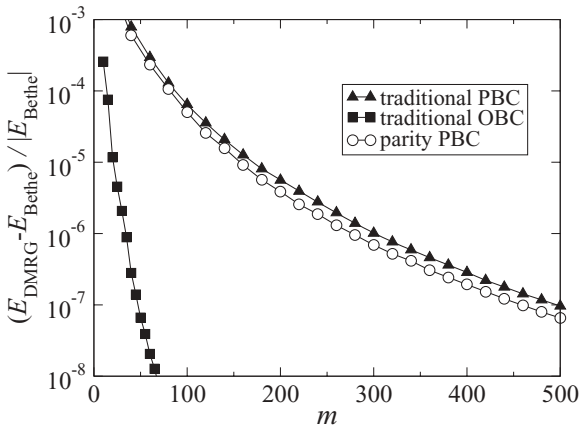

FIG. 8. Relative error in the ground-state energy for a 100 site spin-1/2 Heisenberg chain as a function of the number of states kept m, for periodic and open boundary conditions. E_{DMRG} are computed by use of the finite-system DMRG, and the exact energy E_{Bethe} are obtained from the algebraic Bethe ansatz.[31]

scaling function. The computations in this work were done on the Acer AR585 F1 Cluster of the National Center for High-performance Computing, Taiwan. This work is partially supported by the Hsing Tian Kong Culture & Education Development Foundation. This work is supported by the NSC in Taiwan through Grant No. 100-2112-M-002-013-MY3.

APPENDIX: BOUNDARY CONDITIONS AND PARITY DMRG

In the level spectroscopy (LS) method,[8,9] the TBC and parity quantum numbers are usually required in the numerical algorithm. Although the old parity infinite-system DMRG[24] may obtain accurate energy within the PBC as long as enough large numbers of states are kept, the PBC scheme in Fig. 7(a) cannot be used within TBC because the parity described in Ref. 24 is no longer conserved. Instead of Fig. 7(a), the TBC scheme in Fig. 7(b) should be used. However, it may not be a practical implementation because the direct connection between two blocks slows down the algorithm dramatically.[18] Moreover, the truncation error in the infinite-system DMRG may not reveal the true relative error of energy.[24] It is difficult to evaluate how many states should be kept is enough. These considerations may be the reason why previous LS studies were always performed by use of exact diagonalization.[10–14]

The scheme in Fig. 7(a) was first proposed by White in his initial DMRG papers for PBC.[18] It is known that the traditional DMRG performs worse for PBC. In order to improve the PBC case, the ladder scheme was first proposed by Qin *et al*. in 1995.[45] Unfortunately, this comparison was not published because the ladder scheme did not provide a distinct improvement. Figure 8 shows the comparison of convergence with m for finite-system DMRG. While this parity DMRG within PBC has merely a little superiority to the traditional DMRG, it should be emphasized that the LS method which is based on sine-Gordon theory has a strong numerical tool now.[46] For the PBC case, recent work by Pippan, White, and Evertz shows remarkable improvement with the MPS algorithm. Interested readers may refer to Refs. 47 and 48 for more information.

*d00222009@ntu.edu.tw

[1] V. L. Berezinskii, Sov. Phys. JETP **32**, 493 (1971); J. M. Kosterlitz and D. J. Thouless, J. Phys. C **6**, 1181 (1973).
[2] L. Campos Venuti, C. Degli Esposti Boschi, M. Roncaglia, and A. Scaramucci, Phys. Rev. A **73**, 010303(R) (2006); M. Roncaglia, L. Campos Venuti, and C. Degli Esposti Boschi, Phys. Rev. B **77**, 155413 (2008).
[3] H.-L. Wang, A.-M. Chen, B. Li, and H.-Q. Zhou, J. Phys. A **45**, 015306 (2012); H.-L. Wang, J.-H. Zhao, B. Li, and H.-Q. Zhou, J. Stat. Mech.: Theor. Exp. **(2011)** L10001; B. Wang, M. Feng, and Z.-Q. Chen, Phys. Rev. A **81**, 064301 (2010).
[4] M.-F. Yang, Phys. Rev. A **71**, 030302(R) (2005); Phys. Rev. B **76**, 180403(R) (2007).
[5] Y.-C. Tzeng and M.-F. Yang, Phys. Rev. A **77**, 012311 (2008); Y.-C. Tzeng, H.-H. Hung, Y.-C. Chen, and M.-F. Yang, *ibid*. **77**, 062321 (2008); M. Thesberg and E. S. Sørensen, Phys. Rev. B **84**, 224435 (2011).
[6] S. Hu, B. Normand, X. Wang, and L. Yu, Phys. Rev. B **84**, 220402(R) (2011).
[7] S. Rachel, N. Laflorencie, H. F. Song, and K. Le Hur, Phys. Rev. Lett. **108**, 116401 (2012).
[8] K. Nomura, J. Phys. A **28**, 5451 (1995); A. Kitazawa, *ibid*. **30**, L285 (1997).
[9] K. Nomura and A. Kitazawa, J. Phys. A **31**, 7341 (1998).
[10] M. Nakamura, J. Phys. Soc. Jpn. **68**, 3123 (1999); Phys. Rev. B **61**, 16377 (2000); H. Otsuka and M. Nakamura, *ibid*. **71**, 155105 (2005).
[11] W. Chen, K. Hida, and B. C. Sanctuary, J. Phys. Soc. Jpn. **69**, 237 (2000); Phys. Rev. B **67**, 104401 (2003); T. Murashima, K. Hijii, K. Nomura, and T. Tonegawa, J. Phys. Soc. Jpn. **74**, 1544 (2005).
[12] K. Hijii, A. Kitazawa, and K. Nomura, Phys. Rev. B **72**, 014449 (2005); M. Nakamura, Physica B **329**, 1000 (2003); M. Nakamura, T. Yamamoto, and K. Ide, J. Phys. Soc. Jpn. **72**, 1022 (2003); H. Otsuka, Y. Okabe, and K. Okunishi, Phys. Rev. E **73**, 035105(R) (2006).
[13] S. Furukawa, M. Sato, and A. Furusaki, Phys. Rev. B **81**, 094430 (2010).
[14] T. Tonegawa, K. Okamoto, H. Nakano, T. Sakai, K. Nomura, and M. Kaburagi, J. Phys. Soc. Jpn. **80**, 043001 (2011).
[15] H.-Q. Lin, Phys. Rev. B **42**, 6561 (1990); K. Adegoke and H. Büttner, Chin J. Phys. **48**, 493 (2010).
[16] H. Guo and S.-Q. Shen, Phys. Rev. B **84**, 195107 (2011).
[17] Such an algorithm is also helpful for recent development of classification of symmetry protected topological phases in 1D; see X. Chen, Z.-C. Gu, and X.-G. Wen, Phys. Rev. B **83**, 035107 (2011); **84**, 235128 (2011); X.-G. Wen, *ibid*. **85**, 085103 (2012); Z.-C. Gu and X.-G. Wen, *ibid*. **80**, 155131 (2009) arXiv:1201.2648; E. Tang and X.-G. Wen, arXiv:1204.0520; F. Pollmann, A. M. Turner, E. Berg, and M. Oshikawa, *ibid*. **81**, 064439 (2010); F. Pollmann and A. M. Turner, arXiv:1204.0704.
[18] S. R. White, Phys. Rev. Lett. **69**, 2863 (1992); Phys. Rev. B **48**, 10345 (1993).
[19] S. R. White, Phys. Rev. Lett. **77**, 3633 (1996).
[20] S. R. White, Phys. Rev. B **72**, 180403(R) (2005).
[21] U. Schollwöck, Rev. Mod. Phys. **77**, 259 (2005); K. A. Hallberg, Adv. Phys. **55**, 477 (2006).
[22] S. Yan, D. A. Huse, and S. R. White, Science **332**, 1173 (2011).
[23] I. P. McCulloch and M. Gulácsi, Aust. J. Phys. **53**, 4 (2000); Philos. Mag. Lett. **81**, 447 (2001); Europhys. Lett. **57**, 852 (2002); D. Zgid and M. Nooijen, J. Chem. Phys. **128**, 014107 (2008).
[24] E. S. Sørensen, J. Phys.: Condens. Matter **10**, 10655 (1998).
[25] S. Ramasesha, S. K. Pati, H. R. Krishnamurthy, Z. Shuai, and J. L. Brédas, Phys. Rev. B **54**, 7598 (1996).
[26] S. Rommer and S. Östlund, Phys. Rev. B **55**, 2164 (1997).
[27] I. P. McCulloch, J. Stat. Mech.: Theor. Exp. **(2007)** P10014; U. Schollwöck, Ann. Phys. **326**, 96 (2011).
[28] A. Weichselbaum and S. R. White, Phys. Rev. B **84**, 245130 (2011).
[29] M. Oshikawa, J. Phys.: Condens. Matter **4**, 7469 (1992).
[30] C. N. Yang and C. P. Yang, Phys. Rev. **150**, 321 (1966); M. Gaudin, Phys. Rev. A **4**, 386 (1971).

[31]F. C. Alcaraz, M. N. Barber, M. T. Batchelor, R. J. Baxter, and G. R. W. Quispel, J. Phys. A **20**, 6397 (1987); V. Murg, V. E. Korepin and F. Verstraete, arXiv:1201.5627.

[32]T. Hirano, H. Katsura, and Y. Hatsugai, Phys. Rev. B **77**, 094431 (2008).

[33]H.-C. Jiang, S. Rachel, Z.-Y. Weng, S.-C. Zhang, and Z. Wang, Phys. Rev. B **82**, 220403(R) (2010).

[34]J. Zang, H.-C. Jiang, Z.-Y. Weng, and S.-C. Zhang, Phys. Rev. B **81**, 224430 (2010).

[35]D. Zheng, G.-M. Zhang, T. Xiang, and D.-H. Lee, Phys. Rev. B **83**, 014409 (2011).

[36]H.-H. Tu and R. Orús, Phys. Rev. B **84**, 140407(R) (2011).

[37]F. Pollmann, E. Berg, A. M. Turner, and M. Oshikawa, Phys. Rev. B **85**, 075125 (2012).

[38]J. Lou, S. Qin, and Z. Su, Phys. Rev. B **62**, 13832 (2000); F. Heidrich-Meisner, I. A. Sergienko, A. E. Feiguin, and E. R. Dagotto, *ibid.* **75**, 064413 (2007); Y. Zhao, S.-S. Gong, W. Li, and G. Su, Appl. Phys. Lett. **96**, 162503 (2010).

[39]P. Chen, Z.-L. Xue, I. P. McCulloch, M.-C. Chung, and S.-K. Yip, Phys. Rev. A **85**, 011601(R) (2012); H. Nonne, P. Lecheminant, S. Capponi, G. Roux, and E. Boulat, Phys. Rev. B **84**, 125123 (2011).

[40]F. D. M. Haldane, Phys. Lett. A **93**, 464 (1983); Phys. Rev. Lett. **50**, 1153 (1983).

[41]S. Qin, X. Wang, and L. Yu, Phys. Rev. B **56**, R14251 (1997); S. Qin, Y.-L. Liu, and L. Yu, *ibid.* **55**, 2721 (1997); X. Wang, S. Qin, and L. Yu, *ibid.* **60**, 14529 (1999); S. Qin, J. Lou, L. Sun, and C. Chen, Phys. Rev. Lett. **90**, 067202 (2003).

[42]U. Schollwöck and T. Jolicœur, Europhys. Lett. **30**, 493 (1995).

[43]U. Schollwöck, O. Golinelli, and T. Jolicœur, Phys. Rev. B **54**, 4038 (1996).

[44]H. Aschauer and U. Schollwöck, Phys. Rev. B **58**, 359 (1998).

[45]S. Qin, S. Liang, Z. Su, and L. Yu, Phys. Rev. B **52**, R5475 (1995); M. Kumar, S. Ramasesha, and Z. G. Soos, *ibid.* **79**, 035102 (2009).

[46]The parity DMRG proposed in this paper is not an improvement for the PBC algorithm. However, it provides an easy way to obtain accurate results with parity quantum numbers for large sizes. This parity DMRG may not be the most efficient algorithm, but it is the only reliable parity algorithm beyond exact diagonalization.

[47]F. Verstraete, D. Porras, and J. I. Cirac, Phys. Rev. Lett. **93**, 227205 (2004).

[48]P. Pippan, S. R. White, and H. G. Evertz, Phys. Rev. B **81**, 081103(R) (2010).